creative commons
COMMONS DEED

저작자표시-비영리-변경금지 2.0 대한민국

이용자는 아래의 조건을 따르는 경우에 한하여 자유롭게

- 이 저작물을 복제, 배포, 전송, 전시, 공연 및 방송할 수 있습니다.

다음과 같은 조건을 따라야 합니다:

저작자표시. 귀하는 원저작자를 표시하여야 합니다.

비영리. 귀하는 이 저작물을 영리 목적으로 이용할 수 없습니다.

변경금지. 귀하는 이 저작물을 개작, 변형 또는 가공할 수 없습니다.

- 귀하는, 이 저작물의 재이용이나 배포의 경우, 이 저작물에 적용된 이용허락조건을 명확하게 나타내어야 합니다.
- 저작권자로부터 별도의 허가를 받으면 이러한 조건들은 적용되지 않습니다.

저작권법에 따른 이용자의 권리는 위의 내용에 의하여 영향을 받지 않습니다.

이것은 이용허락규약(Legal Code)을 이해하기 쉽게 요약한 것입니다.

Disclaimer

dCollection

연세대학교
YONSEI UNIVERSITY

An Efficient System for Intestinal On-site Butyrate Production Using Novel Microbiome-Derived Esterases

Dah Hyun Jung

Department of Medicine or Medical Science

The Graduate School, Yonsei University

연세대학교
YONSEI UNIVERSITY

An Efficient System for Intestinal On-site Butyrate Production Using Novel Microbiome-Derived Esterases

Directed by Professor Sang Sun Yoon

The Master's Thesis
the Department of Medical Science,
the Graduate School of Yonsei University
in partial fulfillment of the requirements for the degree
of Master of Medical Science

Dah Hyun Jung

December 2020

연세대학교
YONSEI UNIVERSITY

This certifies that the Master's Thesis of
Dah Hyun Jung is approved.

Thesis Supervisor : Sang Sun Yoon

Thesis Committee Member#1: Soon-Jung Park

Thesis Committee Member#2: Jae Hee Cheon

The Graduate School
Yonsei University

December 2020

연세대학교
YONSEI UNIVERSITY

ACKNOWLEDGEMENTS

석사과정 동안 아낌없이 도움 주시고, 격려해주신 윤상선 교수님께 진심으로 감사드립니다. 교수님께서 항상 믿어주시고, 지지해주신 덕분에 제 연구에 확신을 가지고 나아갈 수 있었습니다. 모든 연구를 열정적으로 마주하시는 교수님의 모습이 저에게 큰 본보기가 되었습니다.

심사위원 박순정 교수님과 천재희 교수님께도 감사의 마음을 전합니다. 바쁘신 와중에도 좋은 연구가 될 수 있도록 조언해 주셔서 진심으로 감사드립니다.

실험이나 진로로 고민할 때 항상 귀기울여 주시고, 조언해주신 이강무 박사님, 윤미영 박사님 그리고 김지은 박사님께도 감사드립니다. 또한 가장 든든한 동기였던 지현 언니, 부족한 동기인데도 잘 챙겨줘서 고마워. 친언니처럼 항상 챙겨주는 진선쌤, 화영쌤, 윤이쌤, 그리고 듬직한 오빠들 광희쌤, 원태쌤, 찬민쌤, 경배쌤, 모하메드, 잘 풀릴 일만 남은 구오즈 채영이, 준범이 그리고 분위기 메이커 리나쌤! 모두 감사합니다.

그리고 항상 전적으로 지지해주는 사랑하는 아빠, 엄마, 그리고 언니. 많이 투덜대는데도 늘 걱정해주고 보살펴주셔서 감사합니다. 모든 분들의 도움으로 제가 여기까지 올 수 있었습니다. 앞으로도 열심히 하는 모습으로 보답하겠습니다. 감사합니다.

2020년 12월
정다현 올림

연세대학교
YONSEI UNIVERSITY

TABLE OF CONTENTS

연세대학교
YONSEI UNIVERSITY

LIST OF FIGURES

LIST OF TABLES

연세대학교
YONSEI UNIVERSITY

ABSTRACT

An Efficient System for Intestinal On-site Butyrate Production Using Novel Microbiome-Derived Esterases

Dah Hyun Jung

Department of Medical Science
The Graduate School, Yonsei University

(Directed by Professor Sang Sung Yoon)

Short-chain fatty acids, especially butyrate, play beneficial roles in sustaining gastrointestinal health. However, due to limitations associated with direct consumption of butyrate, there has been interest in using prodrugs of butyrate. Tributyrin (TB), a triglyceride composed of three butyrate molecules and a glycerol, is a well-studied precursor of butyrate. We screened a metagenome library consisting of 5,760 bacterial artificial chromosomes clones, with DNA inserts originating from mouse microbiomes, and identified two clones that efficiently hydrolyse TB into butyrate. Nucleotide sequence analysis indicated that inserts in these two clones are derived from unknown microbes. BLASTp analysis, however, revealed that each insert contains a gene homologous to acetylesterase or esterase genes, from Clostridium spp. and Bacteroides spp., respectively. Predicted structures of these two proteins both contain serine-histidine-aspartate catalytic triad, highly conserved in the

연세대학교
YONSEI UNIVERSITY

family of esterases. Escherichia coli host expressing each of the two candidate genes invariably produced greater amounts of butyrate in the presence of TB. Importantly, administration of TB together with cloned E. coli cells alleviated inflammatory symptoms in a mouse model of acute colitis. Based on these results, we established an efficient on-site and real-time butyrate production system that releases butyrate in a controlled manner inside the intestine.

Key words: tributyrin, butyrate, esterase, microbiome, gut health

연세대학교
YONSEI UNIVERSITY

An Efficient System for Intestinal On-site Butyrate Production Using Novel Microbiome-Derived Esterases

Dah Hyun Jung

Department of Medical Science
The Graduate School, Yonsei University

(Directed by Professor Sang Sung Yoon)

I. INTRODUCTION

Our immanent symbiont, the intestinal microbiome, has been intensely studied due to its realised impact on human physiology. Dysbiosis of commensal bacteria and alteration of commensal-derived metabolites in the gut trigger greater vulnerability to pathogenic infections, inappropriate immune response or even systematic disorders [1]. Among various bacterial metabolites produced in the gut, short chain fatty acids (SCFAs) are mainly produced by anaerobic fermentation of indigestible polysaccharides by commensal anaerobes, and SCFAs have been highlighted as a key factor for sustaining gut homeostasis [2]. In particular, butyrate, one of the major SCFAs in the gastrointestinal tract, serves as a major energy source for colonocytes and also a signalling molecule as histone deacetylase inhibitor and a ligand of GPR41 or GPR43 receptor [3,4]. Ultimately, butyrate can enhance the gut barrier function

연세대학교
YONSEI UNIVERSITY

of intestinal epithelial cells, exert anti-inflammatory effects, and suppress the occurrence of colorectal cancer [5–7].

Inflammatory bowel disease (IBD), of which major subtypes are ulcerative colitis (UC) and Crohn's disease (CD), is a chronic and relapsing inflammatory condition in the gastrointestinal tract accompanied by persistent diarrhoea, abdominal pain, rectal bleeding, and weight loss [8]. Though the exact trigger of IBD remains unclear, many research indicate that IBD is a result of inappropriate immune response in genetically susceptible individuals [9].

Emerging evidence strongly suggests that dysbiosis of the gut microbiome and IBD are highly correlated, demonstrated by the compositional differences between the stool samples of IBD patients and healthy controls [10]. A significant change of microbial diversity in the IBD stool samples is decreased abundance of Ruminococcaceae (Clostridium cluster IV) and Lachnospiraceae (Clostridium cluster XIVa) [10,11], which are famous butyrate-producing bacteria, compared to stool samples from healthy individuals[12]. Depletion of butyrate in IBD patients might be related to the decreased abundance of butyrate-producing bacteria [13]. Thus, administering either the butyrate-producing bacteria or butyrate itself has been considered as a potential therapeutic agent for the treatment of IBD via its anti-inflammatory effects [14–16].

연세대학교
YONSEI UNIVERSITY

In spite of the prominent therapeutic potential of butyrate, its actual usage in the clinical setting has been met with scepticism due to the short half-life of butyrate. For instance, when butyrate was intravenously administered to a child with leukaemia (500 mg/kg body weight per day) over a period of several days, limited change in prognosis was made, on the account of the short half-life of butyrate of 6 minutes, and low peak serum levels of butyrate observed [17]. Similarly, a separate study measured the blood concentrations of butyrate, and showed a rapid elimination following the intravenous injection of arginine butyrate [18]. Moreover, clinically utilizing dietary fibre as major source of butyrate also seems infeasible. The estimated amount of dietary fibre required to observe clinical efficacy for an average individual is 136 g per 1,000 kcal, which is approximately 9.7 times more than that of the recommended intake of 14 g per 1,000 kcal [19].

In order to overcome this issue of butyrate administration, there has been growing interest in utilizing butyrate derivatives or prodrugs which are more stable and thus more of the administered drug reaches the target site. One of the most prominent prodrugs of butyrate is tributyrin (TB), which is a triglyceride composed of three butyric acid molecules and a glycerol. Butter is one of the richest dietary sources of TB, containing up to 3–4 % of its weight [20]. When TB is ingested, for example through consumption of butter, it gets degraded by hepatic lipases releasing 3 butyrate molecules. Thus, dietary intake of TB is

연세대학교
YONSEI UNIVERSITY

expected to yield similar beneficial results as direct consumption of butyrate. A pharmacokinetic study of TB shows that the plasma half-life of butyrate after TB administration is 40 minutes, which is longer than that of direct butyrate administration [20]. Furthermore, many studies have shown that TB reduces the level of pro-inflammatory cytokines, induces apoptosis of colonic cancer cells similarly to butyrate [21]. *In vivo* experiment using a rat model of colon carcinogenesis also showed that TB exerts anti-cancer effects [22].

We hypothesized that gut commensal microbes may play a role in TB metabolism and that the resulting metabolites, especially butyrate, may provide health benefits to host. In this research, we screened a metagenomic library constructed using the mouse gut commensal microbiome and identified two novel esterase genes whose products efficiently breakdown TB into butyrate. Finally, we tested the anti-inflammatory effects of the combination of TB and commensal *Escherichia coli* clones that express the esterase genes in dextran sulphate sodium (DSS)–induced colitis mouse model.

연세대학교
YONSEI UNIVERSITY

II. MATERIALS AND METHODS

1. Bacterial strains and culture conditions

The procedure for BAC (Bacterial Artificial Chromosome) library construction was described in detail elsewhere [23]. Briefly, bacterial DNA was extracted from the combined caecal and colon contents of seven BALB/c mice and digested with HindIII restriction enzyme. The size-selected DNA was cloned into pIndigoBAC-5 (HindIII cloning-ready; Epicentre), and transformed into *E. coli* DH10B. Successfully transformed *E. coli* DH10B was grown in Luria Broth (LB, 10 g tryptone, 5 g NaCl, 5 g yeast extract per litre) supplemented with 25 μg/ml of chloramphenicol (Duchefa Biochemie, Haarlem, Netherlands) at 37 °C. The indigenous non-pathogenic *E. coli* strains t*Ec* (typical *E. coli*) was isolated from CD-1 mouse intestines in a previous study [24]. This information is summarised in Table 1.

연세대학교
YONSEI UNIVERSITY

Table 1. Bacterial strains and plasmids used in this study

Strains and plasmids	Relevant characteristic	Source
***E. coli* strains**		
DH10B	pIndigoBAC-5 without inserted gene	Laboratory collection
BAC library	DH10B, pIndigoBAC-5 harboring BALB/c mouse gut microbiome DNA	Reference[23]
t*Ec*	wild type strain isolated from CD-1 mouse intestines	Reference[24]
tbe1	t*Ec*, pBAD24::*tbe1*	This study
tbe2	t*Ec*, pBAD24::*tbe2*	This study
Plasmids		
pIndigoBAC-5	Cm^r, library backbone vector	Laboratory collection
pBAD24	Amp^r, cloning vector	Laboratory collection

연세대학교
YONSEI UNIVERSITY

2. Screening of BAC library clones for TB degrading ability

For TB degradation assay, bacteria were grown on TB agar (TBA; 4 g peptone, 3 g NaCl, 3 g yeast extract, 15 g agar, 20 mM TB per litre and 0.02% of triton X-100 as a surfactant) at 37 °C for 48 hours. As TB in the media gets degraded by the hydrolytic activity of bacteria, distinct clear zones form around the bacterial colonies.

3. Measurement of butyrate

Bacteria were inoculated into 3 ml of TB broth (TBA without agar) within 50 ml conical tubes and incubated at 37 °C for 24 hours. TB concentrations used for the initial screening of the metagenomic library and for confirmation of successfully transformed t*Ec* clones were 20 mM and 5 mM, respectively. Bacterial culture supernatants were filtered using 0.2 μm Minisart® Syringe Filters (Sartorius, Germany). Butyrate concentration was measured by high-performance liquid chromatography (HPLC) using Ultimate3000 (Thermo Dionex, USA) with a UV detector (210 nm) and refractive index detector (RefractoMAX520, Japan). For analysis, the Aminex 87H column (300x10 mm, Bio-Rad, USA) was used and 0.01 N H_2SO_4 were used as an eluent.

4. Sequence analysis of the inserted fragments of 33E2 and 54E5

Whole genome sequencing and *de novo* assembly of BAC plasmids were performed by Macrogen, Inc. (Seoul, Korea). ORFs were detected using the

연세대학교
YONSEI UNIVERSITY

ORFfinder provided by the National Center of Biotechnology Information (NCBI). Sequence homology searches were performed against the NCBI database using BLASTn and BLASTp algorithms. ORFs were confirmed with Prokka [25], and any candidates without significant hits with BLASTp were excluded from analysis. Conserved domain search was done by using InterPro database and signal peptide sequence of protein was predicted based on SignalP 5.0 [26].

5. Construction of *E. coli* heterologously expressing *tbe1* and *tbe2*

pBAD24 with an ampicillin resistance marker was used to construct the protein expression vectors (Table 1). The DNA fragment of *tbe1* including the endogenous promoter region (~899 bp) was PCR amplified from the 33E2 clone. The DNA fragment of *tbe2* was PCR amplified from 54E5. Since the endogenous promoter region of *tbe2* was not included in the vector of 54E5, the promoter region of *tbe1* was amplified and combined with the amplified fragment of *tbe2* by overlapping PCR (~1,298 bp). PCR products were cloned into the multi-cloning site of the pBAD24, and the cloned vectors, named pBAD24::*tbe1* and pBAD24::*tbe2*, were transformed into *E. coli* DH10B for amplification. Again, the vectors were extracted from *E. coli* DH10B using AccuPrep Plasmid Mini Extraction kit (Bioneer, Daejeon, Korea) and transformed into t*Ec*. PCR primers used for cloning are listed in Table 2.

연세대학교
YONSEI UNIVERSITY

Table 2. Primers used in this study

Gene name	Direction	Primer sequence (5' -3')*
*tbe1*_promoter_XmaI	Forward	ACTGCCCGGGAGGTCTCACGGATTCAGGAA
*tbe1*_XbaI	Reverse	ACTCTCTAGATCATTGCAGCATCCATTTAA
*tbe1*_promoter_XbaI	Forward	ACTCTCTAGATTGTAAATAACTCAGATTTGGT
*tbe1*_protmoter_overlapped	Reverse	AATTTTTTTCATATTTTCCTCCTGGTATTGCG
*tbe2*_overlapped	Forward	CAGGAGGAAAATATGAAAAAAATTCTAATCCT
*tbe2*_PstI	Reverse	ACTCCTGCAGTTATTTCTTGAAAAGTTGAG

* Restriction enzyme recognition sequences and overlapped sequences are underlined

연세대학교
YONSEI UNIVERSITY

6. Dextran sodium sulphate (DSS) mouse model of acute colitis

Acute colitis was induced in 8-week-old female C57BL/6 mice administered 2.5% dextran sodium sulphate (DSS; molecular weight, 36,000–50,000 Da ; MP Biomedicals, OH, USA) in their drinking water for 5 days, which was replaced with normal drinking water for the following 7 days. The mice were monitored daily for body weight, stool consistency and stool bleeding. Disease activity index (DAI) scores were taken in accordance with a previous study [27]. Over the 7-day period following the DSS administration, mice were orally dosed with TB (3 g/kg) combined with the respective treatments. The treatments delivered were PBS, t*Ec*-pBAD24 (empty vector), t*Ec*-pBAD24::*tbe1*, and t*Ec*-pBAD24::*tbe2*, respectively. The dosage of each bacterial clones provided in combination with TB were $1x10^8$ CFU. The mice were euthanized by CO_2 on the 12^{th} day of the experiment and colon lengths were measured.

7. Histological analysis

Mouse colons of 3 mm were harvested, opened longitudinally and fixed in 3.7 % formaldehyde. Tissues were paraffin-embedded and 5 μm sections were stained with haematoxylin-eosin (H&E). Slides were analysed using an Olympus Microscope (Mod. U-LH100HG).

연세대학교
YONSEI UNIVERSITY

III. RESULTS

1. Tributyrin (TB) degrading clones exhibited butyrate producing capability

Since TB is an ester derived from a glycerol and 3 molecules of butyrate, we postulated that enzymes that can catabolize TB may produce butyrate. Hence, we sought to establish an efficient screening method for high-throughput identification of bacterial clones that express such TB-degrading enzymes. We took advantage of the fact that agar plates containing dissolved TB (Tributyrin Agar, TBA) appear turbid, and that upon TB degradation, the agar turns transparent. Indeed, we observed that bacterial clones producing TB-degrading enzymes, such as PAO1 strain of *Pseudomonas aeruginosa*, form colonies with halos of a cleared zone on TBA (data not shown). Using this simple yet effective screening scheme (Fig. 1A), we screened a metagenomic library consisting of 5,760 bacterial artificial chromosome (BAC) clones, where each DNA insert was purified from the gut microbiome of BALB/c mice [23]. An *E. coli* DH10B that contains the pIndigoBAC-5 vector with no insert was used as negative control. Two clones (33E2 and 54E5) exhibited prominent halos around the colony on TBA following 48 hours growth (Fig. 1B). These two TB-degrading clones were subsequently isolated and evaluated for butyrate production. Quantitative measurement of butyrate using HPLC implicated that 33E2 and 54E5 produced > 8 times and > 3 times more butyrate, respectively, than the

연세대학교
YONSEI UNIVERSITY

control strain in the presence of 20 mM of the substrate TB. This quantitative butyrate measurement is consistent with what was observed on the TB plate (Fig. 1B). In addition, we also confirmed that overnight cultures of 33E2 and 54E5 produced the characteristic smell which signalled butyrate production.

연세대학교
YONSEI UNIVERSITY

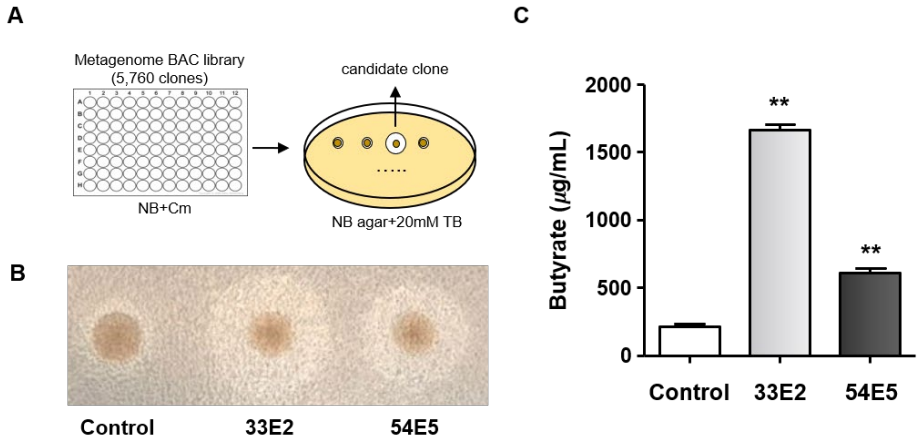

Figure 1. TB degradation of 33E2 and 54E5 clones. (A) Graphical summary of TB esterase screening of BAC library. (B) Representative images of a clear zone formation around TB degrading positive clones, 33E2 and 54E5. *E. coli* DH10B containing pIndigoBAC-5 (vector-only control) is also shown as a control. (C) Measurement of butyrate production by 33E2 and 54E5 in the presence of 20 mM of TB. Three independent experiments were performed, and values (means ± SEM) are displayed in each bar. **, $P < 0.05$ compared to Control.

연세대학교
YONSEI UNIVERSITY

2. Sequence analysis of 33E2 and 54E5 reveals the genes responsible for TB degradation

In order to better understand the genes related to TB degradation, the vectors of 33E2 and 54E5 were sequenced and analysed. Consequently, the sequence of 33E2, which contains a 10.4 kb insert, was fully assembled as a complete circular contig. In contrast, the inserted sequence of the 54E5 clone was assembled as three contigs. Based on the lengths of these three contigs, the insert size of the 54E5 clone is estimated to be larger than 64.7 kb. Full-length sequences of these inserts are currently undergoing the deposition to NCBI database.

When BLASTn searches were performed using the sequences of the 33E2 and 54E5 inserts as query, no significant alignment was retrieved, suggesting that the inserts of these two clones are derived from microbes with unknown genome sequences (Table 3 and Table 4). However, the 33E2 insert is most similar to a region of *Blautia producta* genome with 74.3% identity (Table 3). Third, fourth and fifth highest-ranking hits of the BLASTn search were identified as genomic sequences from *Clostridium lentocellum*, *Herbinix* sp. and *Cellulosilyticum* sp. bacteria, respectively, all of which belong to the Lachnospiraceae family [28,29]. Contig1 and contig3 of the 54E5 insert share regions of high homology with genomic regions of *Duncaniella* sp. (Table 4). No sequence with significant homology to contig2 was detected by BLASTn.

연세대학교
YONSEI UNIVERSITY

Disregarding contig2, most of the hits in Table 4 are associated with members of the Muribaculaceae family [30]. These results suggest that the DNA inserts of 33E2 and 54E5 have originated from bacteria belonging to Lachnospiraceae and Muribaculaceae, respectively. Of note, the predicted origin information of the 33E2 and 54E5 DNA fragments are consistent with the information derived from the BLASTp search of amino acid sequences as query.

The sequence of the 33E2 insert contains 9 ORFs including the first ORF that encodes a putative esterase (Fig. 2A). Although the species origin of the DNA fragment cannot be ascertained, all of the ORFs within the 33E2 insert encode proteins highly homologous to those of Lachnospiraceae family, whose members are well-known producers of short-chain fatty acids [10]. The list of proteins encoded by 33E2 insert genes is provided in Table 5. The protein encoded by ORF1 (795 bp, 240 aa) is most homologous to the alpha/beta hydrolase fold domain-containing protein of *Cellulosilyticum lentocellum* with 60.46% amino acid sequence identity. Second-ranked is a protein with the same description and produced by another species of the same genus, *Cellulosilyticum* (Fig. 2A). Other proteins in the list are acetylesterases, either from the genus of *Clostridium* or *Herbinix* (Fig. 2A). These results strongly suggest that TB-degrading capability of the 33E2 clone can be attributed to the enzymatic activity of this gene product.

연세대학교
YONSEI UNIVERSITY

Table 3. List of BLASTn search results of inserted DNA sequence of 33E2

contig	Rank*	Description	Query Cover	E value	Identity (%)	Accession
33E2	1	*Blautia producta* strain PMF1 chromosome, complete genome	56%	0	74.3	CP035945.1
	2	*Paenibacillus riograndensis* SBR5 genome assembly SBR5(T), chromosome : I	33%	1.00E-80	63.2	LN831776.1
	3	*Clostridium lentocellum* DSM 5427, complete genome	5%	2.00E-34	67.41	CP002582.1
	4	*Herbinix* sp. SD1D genome assembly SD1D, chromosome : I	4%	2.00E-28	67.9	LN879430.1
	5	*Cellulosilyticum* sp. WCF-2 chromosome, complete genome	5%	6.00E-28	66.91	CP034675.1

* Rank of the result is arranged in order of E-value.

연세대학교
YONSEI UNIVERSITY

Table 4. List of BLASTn search results of inserted DNA sequence of 54E5

contig	Rank*	Description	Query Cover	E value	Identity (%)	Accession
54E5 Contig1	1	*Duncaniella* sp. B8 chromosome, complete genome	9%	0	95.53	CP040121.1
	2	*Duncaniella* sp. C9 chromosome	9%	0	95.53	CP039547.1
	3	Muribaculaceae bacterium DSM 108610 strain Oil-RF-744-WCA-WT-10 chromosome, complete genome	9%	5.00E-133	70.62	CP045696.1
	4	*Muribaculum intestinale* strain YL27 chromosome, complete genome	9%	9.00E-143	87.47	CP015402.2
	5	*Muribaculum intestinale* strain YL27 genome	9%	9.00E-143	87.47	CP021421.1
54E5 Contig2	1	Uncultured bacterium clone NOD_dss_A3_G08 16S ribosomal RNA gene, partial sequence	5%	0	99.93	JQ083840.1
	2	Uncultured bacterium clone WT_ctrl_D1_G10 16S ribosomal RNA gene, partial sequence	5%	0	99.87	JQ084982.1
	3	Uncultured bacterium clone NOD_ctrl_C1iii_C05 16S ribosomal RNA gene, partial sequence	5%	0	99.87	JQ084661.1
	4	Uncultured bacterium clone WT_dss_B5_H07 16S ribosomal RNA gene, partial sequence	5%	0	99.87	JQ084456.1
	5	Uncultured bacterium clone WT_dss_B1_C01 16S ribosomal RNA gene, partial sequence	5%	0	99.87	JQ084160.1
54E5 Contig3	1	*Duncaniella* sp. B8 chromosome, complete genome	34%	0	94.98	CP040121.1
	2	*Duncaniella* sp. C9 chromosome	34%	0	94.98	CP039547.1
	3	*Duncaniella dubosii* strain H5 chromosome	33%	0	89.59	CP039396.1
	4	Uncultured bacterium BAC25G1 genomic sequence	26%	0	95.45	KC595277.1
	5	*Muribaculum intestinale* strain YL27 chromosome, complete genome	34%	0	84.81	CP015402.2

*Rank of the result is arranged in order of E-value.

연세대학교
YONSEI UNIVERSITY

The sequence of the 54E5 insert contains 32 ORFs and 90.6% (29 ORFs) of the encoded proteins are highly homologous to proteins from the Bacteroidales order (Fig. 2B). The very first gene in contig3 (1194 bp, 397aa) was determined to encode a protein, whose amino acid sequence is highly homologous to a Muribaculaceae bacterium esterase with 86.9% identity. Proteins retrieved from the BLASTp search using this protein as query similarly include esterases or alpha/beta hydrolases from species of the *Bacteroides* genus (Fig. 2B). Hereafter, we named ORF1 of 33E2 and ORF1 of the 54E5 contig1 as *tbe1* and *tbe2*, respectively, with tbe standing for "**t**ri**b**utyrin **e**sterase".

연세대학교
YONSEI UNIVERSITY

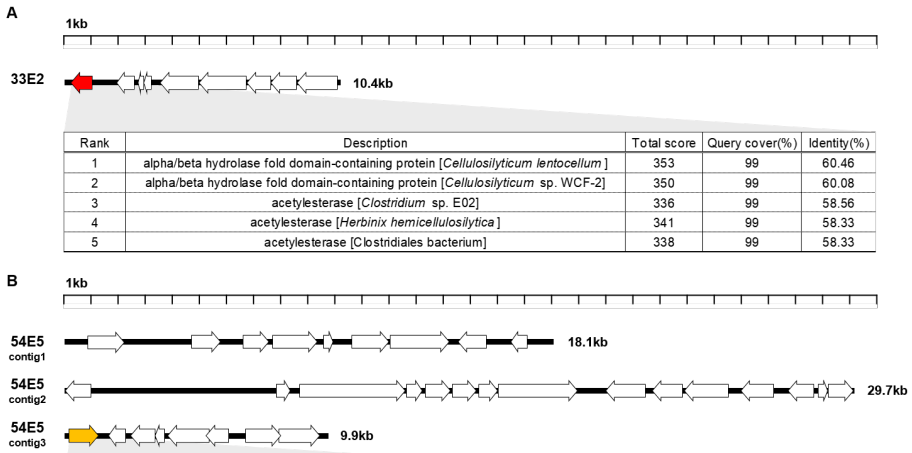

Rank	Description	Total score	Query cover(%)	Identity(%)
1	alpha/beta hydrolase fold domain-containing protein [*Cellulosilyticum lentocellum*]	353	99	60.46
2	alpha/beta hydrolase fold domain-containing protein [*Cellulosilyticum* sp. WCF-2]	350	99	60.08
3	acetylesterase [*Clostridium* sp. E02]	336	99	58.56
4	acetylesterase [*Herbinix hemicellulosilytica*]	341	99	58.33
5	acetylesterase [Clostridiales bacterium]	338	99	58.33

Rank	Description	Total score	Query cover(%)	Identity(%)
1	esterase [Muribaculaceae bacterium]	684	93%	86.9
2	esterase [*Bacteroides rodentium*]	625	94%	78.42
3	alpha/beta hydrolase [*Bacteroides stercorirosoris*]	625	94%	78.16
4	esterase [*Bacteroides* sp. L10-4]	624	94%	78.16
5	esterase [*Bacteroides uniformis*]	624	94%	78.16

Figure 2. Open reading frame (ORF) maps and BLASTp results of 33E2 and 54E5 clones. ORF maps of the (A) 33E2 and (B) 54E5 clones**.** The length and direction of the arrows indicate the relative size and direction of each ORF. Detailed information of the ORFs is described in supplementary information. ORFs encoding putative esterases, Tbe1 and Tbe2, are coloured red and orange, respectively, and the top 5 BLASTp hits of the ORFs are listed in the table arranged by increasing e-value.

연세대학교
YONSEI UNIVERSITY

Table 5. Predicted genes in BAC clones

Clone and ORF(s)	Nucleotide range (start:stop, orientation)	Size of putative protein (amino acids)	Putative function (BLAST hit)	Most similar homologue and Genbank accession no.	Protein sequence identity
33E2, ORF1	1088:294 (-)	240	alpha/beta hydrolase fold domain-containing protein	*Cellulosilyticum lentocellum* WP_013655742.1	Identities=159/263(60%) Positives=204/263(77%)
33E2, ORF2	2704:2045 (-)	219	metallophosphoesterase family protein	Lachnospiraceae bacterium WP_178364842.1	Identities=145/219(66%) Positives=174/219(79%)
33E2, ORF3	3021:2803 (-)	72	hypothetical protein	Lachnospiraceae bacterium HBA67762.1	Identities=47/67(70%) Positives=57/67(85%)
33E2, ORF4	3292:3011 (-)	93	hypothetical protein	Lachnospiraceae bacterium HBA67762.1	Identities=46/79(58%) Positives=58/79(73%)
33E2, ORF5	5083:3665 (-)	472	hypothetical protein (beta fructosidase)	Lachnospiraceae bacterium WP_178780199.1	Identities=377/472(80%) Positives=428/472(90%)
33E2, ORF6	6885:5116 (-)	589	extracellular solute-binding protein	unclassified Lachnospiraceae WP_178780201.1	Identities=494/592(83%) Positives=536/592(90%)
33E2, ORF7	7842:6946 (-)	298	ABC transporter permease subunit	Lachnospiraceae bacterium WP_178780203.1	Identities=272/298(91%) Positives=288/298(96%)
33E2, ORF8	8783:7863 (-)	306	ABC transporter permease subunit	Lachnospiraceae bacterium WP_178780205.1	Identities=275/306(90%) Positives=294/306(96%)
33E2, ORF9	10338:8890 (-)	482	response regulator	Lachnospiraceae bacterium WP_178780207.1	Identities=302/479(63%) Positives=387/479(80%)
54E5_contig1, ORF1	887:2212 (+)	441	anaerobic sulfatase-maturase	uncultured Ruminococcus sp. SCH69572.1	Identities=114/404(28%) Positives=191/404(47%)
54E5_contig1, ORF2	4713:5810 (+)	365	IS110 family transposase	Dysgonomonas gadei WP_006801250.1	Identities=155/363(43%) Positives=224/363(61%)
54E5_contig1, ORF3	6662:7618 (+)	318	IS30 family transposase	Muribaculaceae bacterium WP_123541742.1	Identities=318/318(100%) Positives=318/318(100%)
54E5_contig1, ORF4	7732:9411 (+)	559	hypothetical protein	Prevotella timonensis WP_103002866.1	Identities=263/552(48%) Positives=372/552(67%)
54E5_contig1, ORF5	9620:9982 (+)	120	hypothetical protein	Clostridia bacterium WP_176935933.1	Identities=50/119(42%) Positives=73/119(61%)
54E5_contig1, ORF6	10716:12053 (+)	445	MULTISPECIES: radical SAM protein	Bacteroidales WP_123483718.1	Identities=223/424(53%) Positives=306/424(72%)
54E5_contig1, ORF7	12050:14293 (+)	747	hypothetical protein	Porphyromonas endodontalis WP_004332090.1	Identities=335/727(46%) Positives=463/727(63%)
54E5_contig1, ORF8	15593:14499 (-)	364	tRNA (N6-isopentenyl adenosine(37)-C2)-methylthiotransferase MiaB	Porphyromonadaceae bacterium HAP29096.1	Identities=305/358(85%) Positives=331/358(92%)
54E5_contig1, ORF9	17106:16567 (-)	179	transposase	Bacteroidales bacterium WP_177817021.1	Identities=154/178(87%) Positives=169/178(94%)
54E5_contig2, ORF1	1005:1 (-)	335	hypothetical protein	Muribaculaceae bacterium GFI39866.1	Identities=200/222(90%) Positives=214/222(96%)
54E5_contig2, ORF2	8001:8516 (+)	171	outer membrane beta-barrel protein	Rikenellaceae bacterium WP_178214144.1	Identities=73/154(47%) Positives=101/154(65%)
54E5_contig2, ORF3	8882:12865 (+)	1327	DUF2723 domain-containing protein	unclassified Muribaculaceae WP_123407644.1	Identities=876/1326(66%) Positives=1035/1326(78%)
54E5_contig2, ORF4	12897:13520 (+)	207	polysaccharide deacetylase family protein	Muribaculaceae bacterium WP_123482617.1	Identities=177/206(86%) Positives=194/206(94%)
54E5_contig2, ORF5	13609:14613 (+)	334	NAD-dependent epimerase/dehydratase family protein	Bacteroidales bacterium WP_178233412.1	Identities=238/332(72%) Positives=280/332(84%)
54E5_contig2, ORF6	14610:15536 (+)	308	DUF4271 domain-containing protein	Bacteroidales WP_123482615.1	Identities=158/312(51%) Positives=223/312(71%)
54E5_contig2, ORF7	15600:16373 (+)	257	uroporphyrinogen-III synthase	Bacteroidales WP_123482621.1	Identities=196/250(78%) Positives=226/250(90%)
54E5_contig2, ORF8	16373:19393 (+)	1006	phosphoenolpyruvate synthase	Bacteroidales WP_123482614.1	Identities=826/990(83%) Positives=903/990(91%)
54E5_contig2, ORF9	21846:20353 (-)	497	succinate CoA transferase	Bacteroidales WP_123482612.1	Identities=378/493(77%) Positives=432/493(87%)
54E5_contig2, ORF10	23236:22091 (-)	381	outer membrane beta-barrel protein	unclassified Prevotella WP_172176428.1	Identities=138/389(35%) Positives=207/389(53%)

연세대학교
YONSEI UNIVERSITY

Table 5. (continued)

54E5_contig2, ORF11	24979:23312 (-)	555	hypothetical protein	Bacteroidales bacterium WP_178261924.1	Identities=152/315(48%) Positives=213/315(67%)
54E5_contig2, ORF12	26676:25426 (-)	416	4Fe-4S cluster-binding domain-containing protein	Chryseobacterium sp. WP_089028128.1	Identities=153/404(38%) Positives=235/404(58%)
54E5_contig2, ORF13	28199:27222 (-)	325	IS110 family transposase	Bacteroidales WP_123481028.1	Identities=324/325(99%) Positives=324/325(99%)
54E5_contig2, ORF14	28383:28754 (+)	123	transposase family protein	unclassified Muribaculaceae WP_123612963.1	Identities=123/123(100%) Positives=123/123(100%)
54E5_contig2, ORF15	28768:29694 (+)	308	hypothetical protein	Muribaculaceae bacterium GFI39866.1	Identities=298/308(97%) Positives=303/308(98%)
54E5_contig3, ORF1	51:1244 (+)	397	esterase	Muribaculaceae bacterium WP_172481901.1	Identities=341/397(86%) Positives=367/397(92%)
54E5_contig3, ORF2	2343:1687 (-)	218	transposase	unclassified Muribaculaceae WP_123612964.1	Identities=217/218(99%) Positives=217/218(99%)
54E5_contig3, ORF3	3448:2522 (-)	308	hypothetical protein	Muribaculaceae bacterium GFI39866.1	Identities=299/308(97%) Positives=304/308(98%)
54E5_contig3, ORF4	3833:3462 (-)	123	transposase family protein	unclassified Muribaculaceae WP_123612963.1	Identities=122/123(99%) Positives=122/123(99%)
54E5_contig3, ORF5	5393:4005 (-)	462	NADPH-dependent glutamate synthase	Bacteroidales WP_123481547.1	Identities=412/462(89%) Positives=434/462(93%)
54E5_contig3, ORF6	6240:5386 (-)	284	sulfide/dihydroorotate dehydrogenase-like FAD/NAD-binding protein	Bacteroidales WP_123481546.1	Identities=242/285(85%) Positives=266/285(93%)
54E5_contig3, ORF7	6811:8145 (+)	444	Trk system potassium transporter TrkA	Bacteroidales bacterium WP_177925523.1	Identities=228/446(51%) Positives=304/446(68%)
54E5_contig3, ORF8	8142:9605 (+)	487	TrkH family potassium uptake protein	Bacteroidales bacterium WP_177910348.1	Identities=257/496(52%) Positives=355/496(71%)

연세대학교
YONSEI UNIVERSITY

3. Characterization of Tbe1 and Tbe2

In an effort to shed light on the molecular nature of Tbe1 and Tbe2, the respective amino acid sequences were examined using InterPro and SignalP5.0. Analysis of Tbe1 revealed the lack of a signal peptide in the amino acid sequence implying that Tbe1 is probably an intracellular protein. In contrast, Tbe2 amino acid sequence includes a signal peptide sequence, from residue 1 to 19 (Fig. 3A, red underlined), which suggests that Tbe2 may be an extracellular protein. Furthermore, amino acid sequences of Tbe1 and Tbe2 were compared with those of the known TB esterases, EstA, of *Lactobacillus lactis* and *Streptococcus pneumoniae* [31,32]. All of the proteins contained an alpha-beta hydrolase conserved domain (InterPro entry: IPR029058) which is common to hydrolytic enzymes (Fig. 3A). In addition, we also detected the presence of a serine-histidine-aspartate (SHD) catalytic motif, included within the active sites of most alpha-beta hydrolase fold super family proteins [33] (Fig. 3A). Furthermore, all SHD motifs found in our analysis contained 3 consensus sequences (LLHG, GLSMGG, and DFL) (Fig. 3A, highlighted in black).

We then asked whether Tbe1 and Tbe2 proteins are structurally similar to a known esterase. Structures of Tbe1 and Tbe2 were simulated based on the 3D structure of *S. pneumoniae* EstA [32] from the RSCB Protein Data Bank (PDB entry: 2UZ0) as template. Tbe1 shares the overall structural similarity with the template to a greater extent than Tbe2 does (Fig. 3B). However, the SHD triad,

연세대학교
YONSEI UNIVERSITY

found in both Tbe1 and Tbe2 conserved within the catalytic core region, is nicely superimposed with that of the *S. pneumoniae* esterase. These results strongly suggest that Tbe1 and Tbe2 are responsible for TB degradation and butyrate biosynthesis in the 33E2 and 54E5 clones.

연세대학교
YONSEI UNIVERSITY

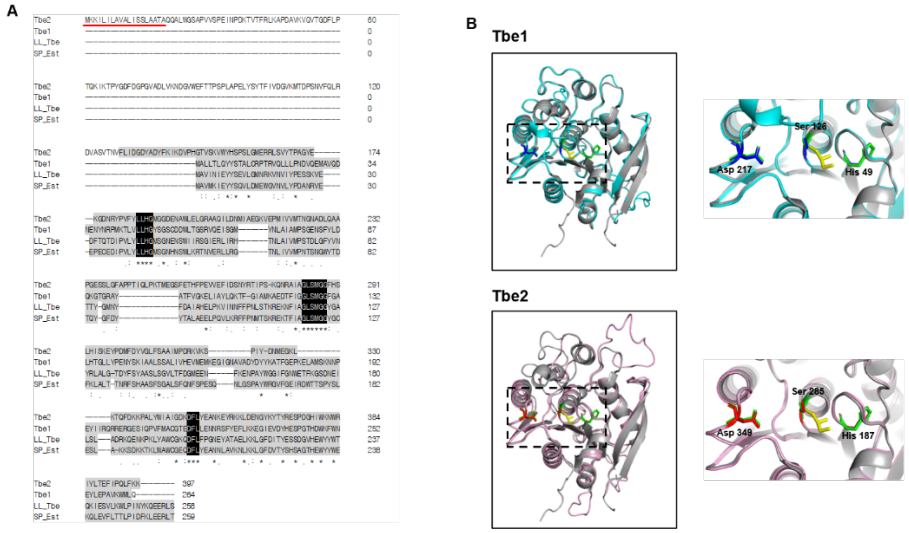

Figure 3. Amino acid sequences and 3-dimensional structures of Tbe1 and Tbe2. (A) Amino acid sequences and multiple amino acid sequence alignment of Tbe1, Tbe2, TB esterase of *L. lactis* (LL_Tbe; UniProtKB Q9L9X0), and esterase of *Streptococcus pneumoniae* (SP_Est; UniProtKB A0A0H2UNZ8). Alpha/beta hydrolase conserved domains and significant consensus sequences are highlighted in grey and black, respectively. Signal peptide is underlined in red. (B) Partial structure of Tbe1 and Tbe2 modelled by SWISS-MODEL. The models are based on the structure of the TB esterase of *Streptococcus pneumoniae* from the RSC Protein Data Bank (2UZ0) as the template. Tbe1, Tbe2, and *S. pneumoniae* TB esterase are shown in cyan, pink, and grey, respectively, with the glycerol residue of TB in yellow. Inside the dotted box is the structure containing the serine-histidine-aspartate (SHD)

연세대학교
YONSEI UNIVERSITY

catalytic triad, as magnified on the right. Each SHD triad of Tbe1, Tbe2 and *S. pneumoniae* tributyrin esterase are shown in blue, red, and green, respectively.

연세대학교
YONSEI UNIVERSITY

4. Tbe1 and Tbe2 degrade TB and produce butyrate

Our bioinformatic analyses clearly suggest that Tbe1 and Tbe2 are the most probable proteins contributing to conversion of TB into butyrate. In order to conclusively determine the roles of Tbe1 and Tbe2, we cloned *tbe1* and *tbe2* genes into another *E. coli* host and monitored TB-induced butyrate production. The host strain we used for Tbe expression is the t*Ec* strain that we isolated from the mouse intestines [24]. *tbe1* gene was amplified to include ~100 bp sequence upstream of the *tbe1* ORF and cloned into pBAD24 plasmid (pBAD24::*tbe1*). Inclusion of the upstream sequence was intended to enable transcription of *tbe1* using its endogenous promoter. *tbe2* gene was inserted right at the junction of the 54E5 plasmid (Fig. 2B), so we were unable to clone *tbe2* with its endogenous promoter. Therefore, *tbe2* gene was cloned in place of the *tbe1* ORF in pBAD24::*tbe1*, and the resultant plasmid was named pBAD24::*tbe2*. When t*Ec* strains harbouring either plasmids were grown in the presence of 5 mM TB, prominent increases in butyrate production level were observed (Fig. 4). Butyrate production levels in these two cultures were >16 times higher than the control culture. The characteristic scent of butyrate was again noticed in these two cultures.

Of interest, the level of butyrate produced by *tbe2* gene was almost identical to that by *tbe1* gene. In Fig. 1C, butyrate production by 54E5 was substantially less than that by 33E2. We speculate that this discrepancy was caused by the

연세대학교
YONSEI UNIVERSITY

absence of *tbe2* gene's own endogenous promoter in the original 54E5 clone. In 54E5, *tbe2* gene expression was probably induced by the upstream sequence part of the pIndigoBAC-5 plasmid. When *tbe2* was transcribed in the presence of the *tbe1* promoter in pBAD24::*tbe2*, greater butyrate production was achieved.

연세대학교
YONSEI UNIVERSITY

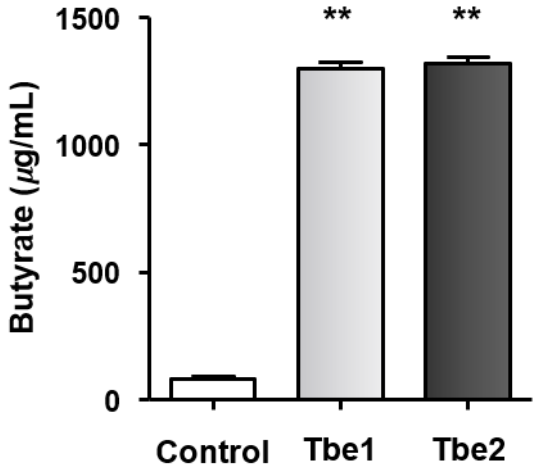

Figure 4. Tbe1 and Tbe2 effectively degrade TB and release butyrate. Measurement of butyrate production by t*Ec* strains harbouring pBAD24::*tbe1* (Tbe1) and pBAD24::*tbe2* (Tbe2) are compared to that of t*Ec* with empty pBAD24 (Control). Bacterial culture was supplemented with 5 mM TB and incubated for 24 hours. Three independent experiments were performed, and values (means ± SEM) are displayed in each bar. **, $P < 0.05$ versus Control.

연세대학교
YONSEI UNIVERSITY

5. *In vivo* on-site butyrate production protects mice against DSS-induced colitis

Our results so far demonstrate that TB together with Tbe-expressing *E. coli* cells can efficiently produce butyrate, a beneficial microbiome-derived metabolite. To examine whether or not butyrate produced by this system can alleviate intestinal inflammation, we used DSS-induced mouse model of acute colitis. Mice were divided into 4 groups that received different treatments, as illustrated in Fig. 5A. Mice administered 2.5 % DSS developed acute colitis characterized by weight loss, bloody diarrhoea, and watery stool, and these outcomes were collectively reflected in the increase of the DAI (Disease Activity Index) score [27] (Fig. 5B). In TB-only group, the DAI scores remained persistently high even after DSS administration was discontinued, suggesting that TB itself did not exert any positive effects toward restoration of a healthy gut condition in mice. It was of particular interest that *E. coli* cells expressing *tbe2* provided significant beneficial effects in mice suffering from severe colitis (Fig. 5B). *E. coli* cells expressing *tbe1* did not seem to confer any protective effects in comparison to the empty vector control group (Fig. 5B). It is not clear why only *tbe2*-expressing *E. coli* cells led to the amelioration of DAI scores.

Another phenotype of the DSS-induced acute colitis is the shortened intestinal length as gut inflammation manifests [34]. On day 12, the last day of the experiment, mice from each group were sacrificed and the lengths of their

연세대학교
YONSEI UNIVERSITY

colons were measured. The colon lengths of mice that received Tbe1- or Tbe2-expressing *E. coli* cells were significantly longer than those of control mice (Fig. 5C), indicating the positive effects of Tbe against DSS-induced colitis. Moreover, the intestinal tissues looked significantly improved by Tbe1 or Tbe2. Hyper-inflammatory responses evidenced by neutrophil infiltration (black arrow) and fluid accumulation (white arrows) were observed in DSS-pretreated mice that received only TB (Fig. 5D). Still higher degrees of neutrophil staining were observed in mice that received control *E. coli* cells (Fig. 5E, black arrow). In contrast, intestinal tissues looked considerably improved when DSS-pretreated mice were treated with TB and *E. coli* cells that express Tbe1 (Fig. 5F) or Tbe2 (Fig. 5G). These results clearly suggest that on-site butyrate production by coupling TB and microbiome-derived novel esterases can exert beneficial effects in the inflamed mouse intestines.

연세대학교
YONSEI UNIVERSITY

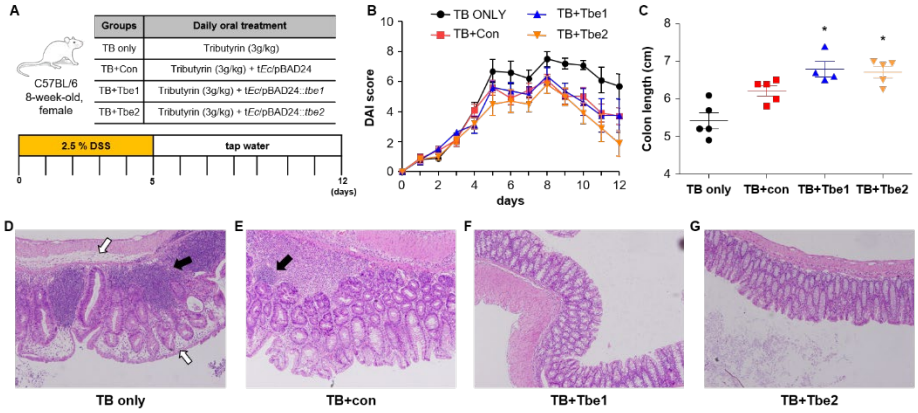

Figure 5. Effects of TB and Tbe on dextran sulphate sodium (DSS)-induced colitis. (A) Schematic diagram of DSS-induced colitis model, (B) disease activity index (DAI) score, and (C) colon length of colitis induced mice treated with only TB (TB ONLY), TB with t*Ec* with empty pBAD24 (TB+Con), t*Ec* with pBAD24::*tbe1* (TB+Tbe1) and t*Ec* with pBAD24::*tbe2* (TB+Tbe2). (D-G) Representative images of H&E stained sections of colons from indicated groups. Arrows denote neutrophil infiltration (black) and edema (white). *, $P < 0.05$ versus TB+Con.

연세대학교
YONSEI UNIVERSITY

IV. DISCUSSION

Though computational analysis has enabled significant progress to be made in recent years, functional metagenomic studies using conventional screening methods still remain irreplaceable and invaluable in the identification of novel genes and characterization of their functions. Metagenomic libraries make it feasible to elucidate the functions of genes from unculturable microbes, which has remained a major challenge in gut microbiome studies. For instance, several niche adaptive features of the gut microbiome such as carbohydrate utilization, colonization factors, bile acid resistance and antibiotic resistance have been revealed through the use of metagenomic libraries constructed from the gut commensal microbiomes of either human or other mammals [35–38].

Since dietary fibres are a major source for SCFAs in our gut, many gut metagenome studies have focused on identifying the genes responsible for the metabolism of dietary fibres [39]. Due to the differences in microbiome compositions among individuals, the level of SCFAs produced from dietary fibres varies significantly [40]. Therefore, it would be of crucial benefit to strategize an efficient system of delivering SCFAs in a controlled manner. Here, we established an on-site butyrate production system (OBPS) using a butyrate precursor and microbiome-derived esterases. We chose TB as a prodrug of butyrate and established a functional metagenome screening method that

연세대학교
YONSEI UNIVERSITY

enabled the identification of genes encoding enzymes that specifically catalyse the conversion of TB to butyrate.

The success of our screening method is attributed to the following elements. Firstly, using Triton X-100, we were able to homogenously solidify agar plates that contain highly insoluble TB. TB agar plates acted as an incredibly useful platform, via which high-throughput screening of a large genomic library was performed with minimal plate-to-plate variations. Secondly, the characteristic scent of butyrate aided the differentiation of positive clones from negative ones, especially during the verification stage. Thirdly, TB is a commonly used substrate in esterase assays, yet previous studies have mostly focused on the enzymes rather than the products of the enzymatic reactions. We focused on the fact that TB is an ester of 3 molecules of butyrate condensed with glycerol, and that positive clones would likely generate butyrate as the major product of TB degradation. Fourthly, TB, as a food-grade lipid, can safely be fed to live animals as a prodrug of butyrate, with no expected side-effects. Thus, TB could be safely administered to experimental animals and enabled *in vivo* confirmation of beneficial effects of TB combined with esterase containing clones.

Until now, TB esterase has gained attention in the context of fermented food and agricultural industries [31,41,42]. Here, we report the discovery of novel esterases in the gut, Tbe1 and Tbe2. These esterases were predicted to have

연세대학교
YONSEI UNIVERSITY

originated from two separate phyla; Firmicutes and Bacteroidetes, two predominant phyla of the human intestine [43]. Given that these phyla are highly abundant and commonly found across individuals irrespective of geography, race, gender and other characteristics, we speculate that this esterase function serves a physiologically significant role and is inherent across a broad spectrum of microbial species in the intestine.

Interestingly, Tbe1 and Tbe2 share a common catalytic feature. Alpha/beta hydrolase domain is highly conserved among various hydrolytic enzymes [44]. Serine residue of the Ser-His-Asp (SHD) catalytic triad, a typical catalytic motif found in the alpha/beta hydrolase domain, is an essential residue for the enzymatic activity of esterases [45] and often included in the consensus sequence (Gly-x-Ser-x-Gly; x refers to any amino acid) [33]. The amino acid sequences of Tbe1 and Tbe2 both contain the sequence GLSMGG which is found in other known TB esterases. The other two residues, histidine and aspartate, are included in the other two consensus sequences, LLHG and DFL, respectively.

The DNA fragment insert of 33E2 is highly homologous to the genome of Lachnospiraceae. Lachnospiraceae is a gram-positive family that belongs to the Firmicutes phylum. Genera such as *Blautia*, *Coprococcus*, *Dorea*, *Lachnospira*, *Oribacterium*, and *Roseburia* are included in this family. Members of Lachnospiraceae are specialised in utilising plant derived-polysaccharides such as starch, inulin, and arabinoxylan [46]. Similar to *Bacteroides* spp. which have

연세대학교
YONSEI UNIVERSITY

well-established carbohydrate utilization systems encoded within polysaccharide utilization loci (PUL), several members of Lachnospiraceae have been reported to possess similar genomic features termed gram-positive PUL (gpPUL). gpPUL is defined as a collection of genes encoding at least one of 3 components: polysaccharide-degrading enzyme, a carbohydrate transport system and a transcriptional regulator [46]. Moreover, esterases are frequently present within a gpPUL. Some ORFs of 33E2 correspond with the 3 components of gpPUL; ORF7 and ORF8 are predicted as ABC transporter permeases, and ORF9 is a response regulator. Hence, it seems highly possible that Tbe1 of 33E2 is involved in carbohydrate degradation of Lachnospiraceae. The carbohydrate degrading ability of Tbe1 may not be limited to TB, but also be extended to include other various polysaccharides, particularly those that are indigestible by host.

In addition, we examined the effects of TB esterase and TB oral supplementation on the gut barrier function in DSS-induced colitis mouse model. TB delivered via the oral route can be hydrolysed by pancreatic and gastric lipases. Hence, many studies have demonstrated that solely administered TB mediates an anti-inflammatory effect. Mounting evidence suggest that supplementation of TB could induce desirable phenotypes in diet-induced obesity model [47], in piglets [48,49], and in a murine model of *Clostridium difficile* infection [50]. In this study, we identified microbiome-derived genes

연세대학교
YONSEI UNIVERSITY

encoding active TB esterases and sub-cloned them into an *E. coli* strain with strong intestinal colonization capability [24]. When those strains were delivered together with TB into the mouse intestines, on-site production of butyrate was achieved. More importantly, thus produced butyrate was sufficient for alleviating the inflammatory symptoms in the mouse model of acute colitis.

In the present study, we report the finding of two novel TB esterases, yet our experiments have the following limitations: (i) the limited amount of information regarding TB esterases present in the gut meant that there was no suitable esterase to compare TB degrading activities of the enzymes to; (ii) TB was the only substrate tested in this study and the substrate specificity of Tbe1 and Tbe2 has not yet been fully explored; (iii) given that Tbe1 likely originated from gram-positive Lachnospiraceae, *E. coli* might not be an appropriate surrogate host for Tbe1 expression; (iv) despite strenuous efforts, we were unable to detect consistently elevated levels of butyrate in mouse faecal matters discharged from groups of TB+Tbe1 or TB+Tbe2. We expect that this can be attributed to the rapid metabolism of butyrate by host colonocytes. Further investigations of real-time butyrate production in mouse intestines are required to better rationalize the therapeutic use of OBPS.

연세대학교
YONSEI UNIVERSITY

V. CONCLUSION

Commercially available probiotics are often limited in that the delivered bacterial strains have difficulty stably colonizing the recipient gut and that sufficient amounts of dietary fibre must be available for bacterial cells to exert beneficial effects. However, the OBPS is advantageous in that it is simple, yet the level of butyrate produced can be controlled by the administrator. Therefore, given the abundant evidence for the significance of butyrate in the maintenance of a healthy gut [5–7], the OBPS may prove to be an invaluable treatment option for various diseases.

연세대학교
YONSEI UNIVERSITY

REFERENCES

1. Maloy KJ, Powrie F. Intestinal homeostasis and its breakdown in inflammatory bowel disease. Nature. 2011.

2. Koh A, De Vadder F, Kovatcheva-Datchary P, Bäckhed F. From dietary fiber to host physiology: Short-chain fatty acids as key bacterial metabolites. Cell. 2016;165:1332–45.

3. Johnstone RW. Histone-deacetylase inhibitors: Novel drugs for the treatment of cancer. Nature Reviews Drug Discovery. 2002.

4. Chang P V., Hao L, Offermanns S, Medzhitov R. The microbial metabolite butyrate regulates intestinal macrophage function via histone deacetylase inhibition. Proc Natl Acad Sci U S A. 2014.

5. Ma X, Fan PX, Li LS, Qiao SY, Zhang GL, Li DF. Butyrate promotes the recovering of intestinal wound healing through its positive effect on the tight junctions. J Anim Sci. 2012.

6. Matter K, Aijaz S, Tsapara A, Balda MS. Mammalian tight junctions in the regulation of epithelial differentiation and proliferation. Current Opinion in Cell Biology. 2005.

7. Gonçalves P, Martel F. Butyrate and Colorectal Cancer: The Role of Butyrate Transport. Curr Drug Metab. 2013.

연세대학교
YONSEI UNIVERSITY

8. Baumgart DC, Carding SR. Inflammatory bowel disease: cause and immunobiology. Lancet. 2007.

9. Zhang YZ, Li YY. Inflammatory bowel disease: Pathogenesis. World J Gastroenterol. 2014.

10. Halfvarson J, Brislawn CJ, Lamendella R, Vázquez-Baeza Y, Walters WA, Bramer LM, et al. Dynamics of the human gut microbiome in inflammatory bowel disease. Nat Microbiol. 2017.

11. Matsuoka K, Kanai T. The gut microbiota and inflammatory bowel disease. Seminars in Immunopathology. 2015.

12. Duncan SH, Barcenilla A, Stewart CS, Pryde SE, Flint HJ. Acetate utilization and butyryl coenzyme A (CoA): Acetate-CoA transferase in butyrate-producing bacteria from the human large intestine. Appl Environ Microbiol. 2002.

13. Marchesi JR, Holmes E, Khan F, Kochhar S, Scanlan P, Shanahan F, et al. Rapid and noninvasive metabonomic characterization of inflammatory bowel disease. J Proteome Res. 2007.

14. Miguel MA, Lee SS, Mamuad LL, Choi YJ, Jeong CD, Son A, et al. Enhancing Butyrate Production, Ruminal Fermentation and Microbial Population through Supplementation with Clostridium saccharobutylicum. J Microbiol Biotechnol. 2019.

연세대학교
YONSEI UNIVERSITY

15. Van Immerseel F, Ducatelle R, De Vos M, Boon N, Van De Wiele T, Verbeke K, et al. Butyric acid-producing anaerobic bacteria as a novel probiotic treatment approach for inflammatory bowel disease. Journal of Medical Microbiology. 2010.

16. Geirnaert A, Calatayud M, Grootaert C, Laukens D, Devriese S, Smagghe G, et al. Butyrate-producing bacteria supplemented in vitro to Crohn's disease patient microbiota increased butyrate production and enhanced intestinal epithelial barrier integrity. Sci Rep. 2017.

17. Novogrodsky A, Dvir A, Ravid A, Shkolnik T, Stenzel KH, Rubin AL, et al. Effect of polar organic compounds on leukemic cells: Butyrate-induced partial remission of acute myelogenous leukemia in a child. Cancer. 1983.

18. Daniel P, Brazier M, Cerutti I, Pieri F, Tardivel I, Desmet G, et al. Pharmacokinetic study of butyric acid administered in vivo as sodium and arginine butyrate salts. Clin Chim Acta. 1989;181:255–63.

19. Macia L, Tan J, Vieira AT, Leach K, Stanley D, Luong S, et al. Metabolite-sensing receptors GPR43 and GPR109A facilitate dietary fibre-induced gut homeostasis through regulation of the inflammasome. Nat Commun. 2015.

20. Newmark HL, Lupton JR, Young CW. Butyrate as a differentiating

연세대학교
YONSEI UNIVERSITY

agent: pharmacokinetics, analogues and current status. Cancer Letters. 1994.

21. Vinolo MAR, Rodrigues HG, Hatanaka E, Sato FT, Sampaio SC, Curi R. Suppressive effect of short-chain fatty acids on production of proinflammatory mediators by neutrophils. J Nutr Biochem. 2011.

22. Heidor R, Furtado KS, Ortega JF, de Oliveira TF, Tavares PELM, Vieira A, et al. The chemopreventive activity of the histone deacetylase inhibitor tributyrin in colon carcinogenesis involves the induction of apoptosis and reduction of DNA damage. Toxicol Appl Pharmacol. 2014.

23. Walter J, Mangold M, Tannock GW. Construction, analysis, and β-glucanase screening of a bacterial artificial chromosome library from the large-bowel microbiota of mice. Appl Environ Microbiol. 2005.

24. Yoon MY, Min KB, Lee KM, Yoon Y, Kim Y, Oh YT, et al. A single gene of a commensal microbe affects host susceptibility to enteric infection. Nat Commun. 2016.

25. Seemann T. Prokka: Rapid prokaryotic genome annotation. Bioinformatics. 2014.

26. Almagro Armenteros JJ, Tsirigos KD, Sønderby CK, Petersen TN, Winther O, Brunak S, et al. SignalP 5.0 improves signal peptide

연세대학교
YONSEI UNIVERSITY

predictions using deep neural networks. Nat Biotechnol. 2019.

27. Chen Y, Si J min, Liu W li, Cai J ting, Du Q, Wang L jing, et al. Induction of experimental acute ulcerative colitis in rats by administration of dextran sulfate sodium at low concentration followed by intracolonic administration of 30% ethanol. J Zhejiang Univ Sci B. 2007.

28. Miller DA, Suen G, Bruce D, Copeland A, Cheng JF, Detter C, et al. Complete genome sequence of the cellulose-degrading bacterium Cellulosilyticum lentocellum. Journal of Bacteriology. 2011.

29. Koeck DE, Maus I, Wibberg D, Winkler A, Zverlov V V., Liebl W, et al. Complete genome sequence of Herbinix luporum SD1D, a new cellulose-degrading bacterium isolated from a thermophilic biogas reactor. Genome Announc. 2016.

30. Lagkouvardos I, Pukall R, Abt B, Foesel BU, Meier-Kolthoff JP, Kumar N, et al. The Mouse Intestinal Bacterial Collection (miBC) provides host-specific insight into cultured diversity and functional potential of the gut microbiota. Nat Microbiol. 2016.

31. Fernández L, Beerthuyzen MM, Brown J, Siezen RJ, Coolbear T, Holland R, et al. Cloning, characterization, controlled overexpression, and inactivation of the major tributyrin esterase gene of Lactococcus

연세대학교
YONSEI UNIVERSITY

lactis. Appl Environ Microbiol. 2000.

32. Tettelin H, Nelson KE, Paulsen IT, Eisen JA, Read TD, Peterson S, et al. Complete genome sequence of a virulent isolate of Streptococcus pneumoniae. Science (80-). 2001.

33. Bornscheuer UT. Microbial carboxyl esterases: Classification, properties and application in biocatalysis. FEMS Microbiology Reviews. 2002.

34. Chassaing B, Aitken JD, Malleshappa M, Vijay-Kumar M. Dextran sulfate sodium (DSS)-induced colitis in mice. Curr Protoc Immunol. 2014.

35. Patrascu O, Béguet-Crespel F, Marinelli L, Le Chatelier E, Abraham AL, Leclerc M, et al. A fibrolytic potential in the human ileum mucosal microbiota revealed by functional metagenomic. Sci Rep. 2017.

36. Yoon MY, Lee KM, Yoon Y, Go J, Park Y, Cho YJ, et al. Functional screening of a metagenomic library reveals operons responsible for enhanced intestinal colonization by gut commensal microbes. Appl Environ Microbiol. 2013.

37. Jones B V., Begley M, Hill C, Gahan CGM, Marchesi JR. Functional and comparative metagenomic analysis of bile salt hydrolase activity in the human gut microbiome. Proc Natl Acad Sci U S A. 2008.

연세대학교
YONSEI UNIVERSITY

38. Cheng G, Hu Y, Yin Y, Yang X, Xiang C, Wang B, et al. Functional screening of antibiotic resistance genes from human gut microbiota reveals a novel gene fusion. FEMS Microbiol Lett. 2012.

39. Tasse L, Bercovici J, Pizzut-Serin S, Robe P, Tap J, Klopp C, et al. Functional metagenomics to mine the human gut microbiome for dietary fiber catabolic enzymes. Genome Res. 2010.

40. de la Cuesta-Zuluaga J, Mueller NT, Álvarez-Quintero R, Velásquez-Mejía EP, Sierra JA, Corrales-Agudelo V, et al. Higher fecal short-chain fatty acid levels are associated with gut microbiome dysbiosis, obesity, hypertension and cardiometabolic disease risk factors. Nutrients. 2019.

41. Faradila S, Oetari A, Sjamsuridzal W. Detection of tributyrin utilization by Rhizopus azygosporus UICC 539 at various temperatures. In: AIP Conference Proceedings. 2020.

42. Esteban-Torres M, Mancheño JM, de las Rivas B, Muñoz R. Production and characterization of a tributyrin esterase from Lactobacillus plantarum suitable for cheese lipolysis. J Dairy Sci. 2014.

43. Arumugam M, Raes J, Pelletier E, Le Paslier D, Yamada T, Mende DR, et al. Enterotypes of the human gut microbiome. Nature. 2011.

44. Ollis DL, Cheah E, Cygler M, Dijkstra B, Frolow F, Franken SM, et al. The alpha/beta hydrolase fold. Protein Eng. 1992.

연세대학교
YONSEI UNIVERSITY

45. Kahya HF, Andrew PW, Yesilkaya H. Deacetylation of sialic acid by esterases potentiates pneumococcal neuraminidase activity for mucin utilization, colonization and virulence. PLoS Pathog. 2017.

46. Sheridan PO, Martin JC, Lawley TD, Browne HP, Harris HMB, Bernalier-Donadille A, et al. Polysaccharide utilization loci and nutritional specialization in a dominant group of butyrate-producing human colonic firmicutes. Microb Genomics. 2016.

47. Sato FT, Yap YA, Crisma AR, Portovedo M, Murata GM, Hirabara SM, et al. Tributyrin Attenuates Metabolic and Inflammatory Changes Associated with Obesity through a GPR109A-Dependent Mechanism. Cells. 2020;9.

48. Sotira S, Dell'Anno M, Caprarulo V, Hejna M, Pirrone F, Callegari ML, et al. Effects of tributyrin supplementation on growth performance, insulin, blood metabolites and gut microbiota in weaned piglets. Animals. 2020.

49. Wang C, Cao S, Shen Z, Hong Q, Feng J, Peng Y, et al. Effects of dietary tributyrin on intestinal mucosa development, mitochondrial function and AMPK-mTOR pathway in weaned pigs. J Anim Sci Biotechnol. 2019.

50. Fachi JL, Felipe J de S, Pral LP, da Silva BK, Corrêa RO, de Andrade

연세대학교
YONSEI UNIVERSITY

MCP, et al. Butyrate Protects Mice from Clostridium difficile-Induced Colitis through an HIF-1-Dependent Mechanism. Cell Rep. 2019.

연세대학교
YONSEI UNIVERSITY

ABSTRACT(IN KOREAN)

장내 미생물 유래 신규 트리뷰트린 에스터레이스를 활용한 효율적인 낙산 생성 시스템 개발

< 지도교수 윤 상 선 >

연세대학교 대학원 의과학과

정 다 현

짧은 사슬 지방산, 특히 낙산은 장 건강을 유지하는 데 유익한 역할을 한다. 그러나, 낙산 직접적인 섭취 시 발생하는 한계점으로 인해, 직접적인 낙산의 사용 대신, 낙산의 prodrug 를 활용하는 방법이 주목되어왔다. 트리뷰티린은 3 개의 낙산 분자와 하나의 글라이세롤로 구성된 트리글리세라이드로 낙산의 선구물질이다. 우리는 쥐의 장내 공생미생물에서 유래한 DNA 를 포함하고 있는 5,760 개의 박테리아 인공 염색체 클론으로 구성된 *Escherichia coli* 메타게놈 라이브러리를 선별해 트리뷰티린을 낙산으로 효율적으로 가수 분해하는 두 개의 클론을 확인했다. 핵산 서열 분석 결과 이 두 클론에 삽입된 DNA 는 알려지지 않은 미생물에서 유래된 것으로 나타났다. 그러나 BLASTp 분석 결과 각각의 삽입 DNA 서열에는 각각 *Clostridium* spp.와 *Bacteroides* spp.의 아세틸에스터레이스 또는 에스터레이스 유전자와 유사한 유전자가

연세대학교
YONSEI UNIVERSITY

포함되어 있는 것으로 밝혀졌다. 이 두 단백질의 예측 3 차원 구조 분석과 아미노산 서열분석을 통해, 두 단백질 모두 에스테라제 계열에서 흔히 보존되어 있는 부위인 세린-히스타딘-아스파테이트 구조를 포함한다는 사실을 발견하였다. 두 후보 유전자를 각각 발현하는 대장균 숙주와 트리뷰티린을 함께 급성 대장염의 마우스 모델에 투여하였을 때, 트리뷰티린 단독 투여 대비 염증 증상을 완화시키는 것을 확인하였다. 이러한 결과를 바탕으로 장내 낙산을 통제 가능한 방법으로 방출하는 효율적인 실시간 낙산 생성 체계를 구축했다.

핵심되는 말: 트리뷰티린, 낙산, 에스터레이스, 공생 미생물, 장건강